Malaysian Journal of Civil Engineering 29 Special Issue (1):37-55 (2017)

BOND PERFORMANCES BETWEEN CFRP PLATE AND STEEL PLATE TO CONCRETE PRISM USING STRUCTURAL ADHESIVES

Nor Izzah Mokhtar[1*], Shukur Abu Hassan[2], Abdul Rahman Mohd. Sam[1], Yusof Ahmad[1] & Balqis Omar[1]

[1]*Department of Structure and Materials, Faculty of Civil Engineering, Universiti Teknologi Malaysia, 81310 Skudai, Johor, Malaysia*
[2]*Centre for Composites (CfC), Institute for Vehicle and System Engineering (IVeSE), Universiti Teknologi Malaysia, 81310 Skudai, Johor Bharu, Malaysia*

*Corresponding Author: *mnorizzah@gmail.com*

Abstract: Repair and rehabilitation of existing structures is a necessity compared to impractical application by direct replacement of the structures. Repair using steel plates to concrete structures had been seen as the most popular method but these techniques had drawn many problems at sites. Recent application of repair and rehabilitation involved externally bonded reinforcement that causing interface performance as an interesting area to be studied. Performance of epoxied system in externally bonded plates needs to examine more to improve database in literature. This study is required to discover the behaviour of interfacial bond in epoxied based. Bonding of external plate to concrete surfaces using adhesive is a practical solution for upgrading the existing reinforced concrete structures. This paper focuses on the bonding performance of epoxy resin adhesives to CFRP-concrete and steel-concrete prisms. Concrete prisms size of 100 × 100 × 300 mm with roughened surface on both sides was prepared. Surface preparation of the concrete prisms was carefully made prior to bonding to CFRP plates and steel plates respectively. Two groups of specimens, namely CFRP Plate-Epoxy-Concrete Prism and Steel Plate-Epoxy-Concrete Prism, were prepared and tested by applying direct tensile loads until failure. The strain distribution along the bond length of the CFRP Plate-Epoxy-Concrete Prism was fairly linear but with further increase of loads, the local strain became non-uniform and non-linear. The strain distribution along the bond length for Steel Plate-Epoxy-Concrete Prism was almost linear, i.e. proportional to the applied load and uniform. The specimen did not failed at the bonding region but failed due to yielding of steel plates. Result from direct tensile test of the steel plates had drawn to conclusion that the strength of steel plates used for this study was not sufficient in term of strength. The test results showed that structural type of epoxide resin was suitable to be used as structural adhesive. The bonding strength was affected by the length of the bonding surface, modulus of elasticity of the materials and interfacial conditions. It is proven by the better performance from CFRP-prism samples with 283.2MPa local bond stress maximum differences if compared with the Steel-prism. Stress concentration was quite close at bond length of 15mm to 35mm. The stresses decreased gradually from bond length of 65mm to 155mm. The longer or wider the bonding surface, the stronger the bonding strength would be but had to be limited to effective bond length of 60 mm to 120 mm of bond length.

Keywords: *Epoxy adhesive bonding, CFRP plate, steel plate, concrete, bond behavior*

1.0 Introduction

Repair and rehabilitation of existing structures has become one of the construction industry major growth areas. Increasing structural load capacity and seismic retrofit of concrete components in earthquake regions is now a substantial part of rehabilitation market (Gao *et al*., 2007). Moreover, transportation infrastructure need to be strengthened to extend the service life and to accommodate the increasing load demand, which is very much higher than that it was first constructed (Christopher, 2006); (Gheorghiu *et al*., 2006); (Gheorghiu *et al*. 2007).

Direct replacement using new structural elements is not practical, thus making repair and rehabilitation a necessity. Among various strengthening and rehabilitation methods developed, externally bonded fibre-reinforced polymer (FRP) materials is an attractive alternatives due to its ease and speed of installation, high durability, corrosion and chemical resistance (Toutanji and Ortiz, 2001); (Wu, Li, and Sakuma, 2006). In the application of externally bonded method, FRP in the form of sheets and plates were bonded to the tension face or shear zone of the structural elements. This method had been proven viable in increasing the flexural and shears performances of reinforced concrete (RC) beams (Khalifa *et al*., 1998); (Abdel-Jaber *et al*., 2003); (Adhikary and Mutsuyoshi, 2004); (Mofidi and Chaallal, 2011); (Dong*et al*., 2013). Researchers had developed analytical solution(Deng *et al*., 2011) and finite element analysis(Deng *et al*., 2011); (De Domenico, 2015) used to evaluate the flexural strength of strengthened structural members.

In most cases, repair and rehabilitation methods involve the use of steel plates. Plates are usually bonded or bolted to the sides of the beams or tension faces. However, these plating techniques consumed times and handling problems at sites. For FRP bolted plated beams, the fracture of bolt shear connectors due to excessive slippage, buckling of plates, splitting and flexural failure are commonly found. On the other hand, the adhesive bonding plates normally result in flexural peeling, shear peeling and axial peeling (Deric J. Oehlers, 2001). Adhesive bonding plates were also subjected to durability problem upon exposure to the surrounding environment(Walker and Hutchinson, 2003). Behaviour of the interfacial bond between the plates and substrate was also investigated by previous studies (Juvandes and Barbosa, 2012); (Daud *et al*., 2015). More studies need to explore the static and fatigue performance of the joints (Daud *et al*., 2015); (Zheng *et al*., 2015). Some of them developed a model to evaluate the debonding mechanism (Xu *et al*., 2015).

Generally, bonded joint is where the surface are held together by means of structural adhesive. This type of joint must satisfy all these conditions to reach its objective correctly; the adhesive should not exceed an allowable shear stress where the performances of the joint depend to the adjustment of the maximum shear stresses to be less than the joint shear strength; the adhesive also not exceed an allowable tensile (peel stress); the adherend is not exceed the through thickness tensile stress allowable; and the adherend must not exceed the allowable in-plane shear stress.

The feasibility of bonding concrete with epoxy resins was first demonstrated in the late 1940s with the early development of structural adhesives reported by Fleming and King (1967). Since the early 1950s adhesives have been used widely in civil engineering and although the building and construction industries represent some of the largest users of adhesive materials, many applications are non-structural in the sense that the bonded assemblies are not used to transmit or sustain significant stresses. Truly structural adhesives imply that the adhesive is used to provide a shear connection between similar or dissimilar materials, enabling the components being bonded to act as a composite structural unit. Such structural applications include the bonding of external plate reinforcement, the shear resistance between the steel and concrete of steel/concrete construction, bonded steelwork details such as cover plates and glue-laminated timber members. There are many advantages of structural adhesives connections such as there are no damage to the parent material (e.g. drilling holes), good aesthetics, improved resistance to corrosion, high effective stiffness to joint, improved fatigue performance, tolerant to dimension inaccuracies, efficient method of joining thin materials and promote simpler and faster fabrication.

Recent application of externally bonded reinforcement had drawn to the increasing study on the interface performance. Many studies had been conducted focusing on bonding strength and performance between FRP and substrate through experimental (Seracino *et al*., 2007); (Kotynia, 2012); (Burke *et al*., 2013); (Wang*et al*., 2014); (Abu Hassan*et al*., 2015); (Firmo *et al*., 2015); (Kalfat and Al-Mahaidi, 2015) guidelines (Grande *et al*., 2011), finite element analysis(Khelifa *et al*., 2015) and analytical analysis (Ko *et al*., 2014); (Al-Saawani*et al*., 2015); (Biscaia *et al*., 2015). Some models were used to test the precision of codes and standard available on the prediction of intermediate crack debonding behaviour of the adhesion joints (Al-Saawani *et al*., 2015). Recent study had explored the application of roughing material replacing adhesive joint between FRP sheets to concrete(Wang *et al*., 2014). Interfacial bond in extreme environmental conditions between FRP and concrete is important as these circumstances had least reported in literature(Abu Hassan *et al*., 2015). Performance of epoxied system in externally bonded plates needs to examine more aspects to improve database in literature. Therefore, this study is required to investigate the behaviour of interfacial bond in epoxied based. This paper presents the study on the bonding behavior of epoxy resin adhesives to CFRP-concrete and steel-concrete.

2.0 Methodology

This section briefly describes the methods used in test samples casting and design parameters, preparation and test method. Figures were attached for better understanding. In this study, the test samples of CFRP plate-epoxy-concrete prisms and steel plate-epoxy-concrete prisms were prepared and tested to failure.

2.1 Concrete Prisms Specifications

The concrete mix proportion used to cast all beams was according to British method of concrete mix design or popularly referred as DoE method and the concrete strength was set to be Grade 40. The concrete mix design details are shown in Table 1. The overall dimensions of concrete prism were pre-determined to be 100 × 100 × 300 mm.

Sieve analysis of aggregates, trial mix and slump test were carried out before the actual concrete mixing process in order to assure concrete quality. Concrete batch was prepared by using drum mixer and fresh concrete was poured into the formwork that had been prepared earlier. The prisms were compacted by using poker vibrator. Nine cube specimens were prepared for every batch of concrete. As a standard practice, the cast concrete cubes with the size of 100 mm x 100 mm x 100 mm have undergone compression tests at the ages of 7, 28 and 90 days to evaluate the compressive strength characteristics. All specimens and concrete prisms were immersed in water tank for 21 days and left to air dried for curing to obtain the desired strength until the next preparation work. Figure 1 shows the formworks for concrete prisms and Figure 2 shows the hardened concrete prisms left for curing.

Table 1**:** DoE Mix Design Summary

Stage	Item	Values
1	1.1 Characteristic strength	40 N/mm^2 (28 days)
	1.2 Target mean strength	53.12 N/mm^2
	1.3 Water-cement ratio	0.46
2	2.1 Slump or Vebe time	100 mm
	2.2 Max aggregate size	10 mm
	2.3 Free-water content	250 kg/m^3
3	3.1 Cement content	543 kg/m^3
4	4.1 Assumed relative density of aggregate	2.65
	4.2 Concrete density (assumed)	2320 kg/m^3
	4.3 Aggregate content	1527 kg/m^3
5	5.1 Fine aggregate content	840 kg/m^3
	5.2 Coarse aggregate content	687 kg/m^3

Figure 1: Formwork for concrete prisms

Figure 2: Concrete prisms left for curing

Table 2 shows the compression test results of concrete test cubes. The specimens were tested under compressive load at loading rate of 2 kN/s in accordance to BS EN 12390-3: 2009(British Standard Institution, 2009).The means compressive strength at 7, 28 and 90 days were 48.6 MPa, 54.9 MPa and 67.4 MPa respectively.

Table 2: Compressive strength of concrete cubes

Compressive Strength Test									
Days		7			28			90	
Batch	1	2	3	1	2	3	1	2	3
Load, kN	497.7	453.0	507.0	558.3	520.0	567.7	676.7	671.3	675.0
Strength, N/mm^2	49.8	45.3	50.7	55.8	52.0	56.8	67.7	67.1	67.5
Average Strength		48.6			54.9			67.4	

2.2 Concrete Surface Preparation

Initially, concrete prisms with good surface quality were chosen. The margins or borders of the bonding area were marked using masking tape. For the CFRP and steel plates, the bonding length is 50 mm and 200 mm respectively. Before the hacking process to roughen the concrete surface was carried out, one of the bonding edge was installed with a 10 mm steel plate, attached using G-clamp. This was to protect the concrete edge from peeling off during the hacking process using air tool hammer and the depth of the hacked surface was around 2 mm. The preparation process of the concrete surface is shown in Figures 3 and 4.

Figure 3: Hacking using air tool hammer

Figure 4: Hacked concrete surfaces

2.3 Plates Specifications

A CFRP plate was produced using Pultrusion technology which consists of high strength unidirectional carbon fibre imbedded with vinyl ester resin matrix. This material was classified as Carbon fibre type S (high strength) came in a roll form. The plate dimensions used in the test were 1.5 mm thick by 50 mm width and 555 mm long. Their mechanical properties of the CFRP plate are shown in Table 3.

Table 3: Typical mechanical properties of CFRP Plate(Hassan, 2007)

	Tensile strength (MPa)	Tensile modulus (GPa)	Longitudinal tensile strain at ultimate (με)	Transverse tensile strain at ultimate (με)	Poisson's ratio (υ)	Fibre volume (%)
Laboratory Test	2,409	135	18,500	3,850	0.28	na

2.*4 Plates Preparations*

Both sides of the CFRP plate are laminated with a protection layer. After the cutting process, the protective layers need to be peeled off. The peeling processes are as shown in Figure 5. Mild steel end tab plate was bonded on both sides at the end of each CFRP plate using Sikadur-30 epoxy adhesive. After the end tabs bonding process is completed, the test specimen was left in the control room for at least three days. The mild steel tab/CFRP plates had to be drilled to provide assessment of the pulling bolt. Similar to CFRP plate, the steel plate is also 555 mm in length. The steel plate bond surface was sandblasted in order to remove the coating surface before bonded to the concrete surface.

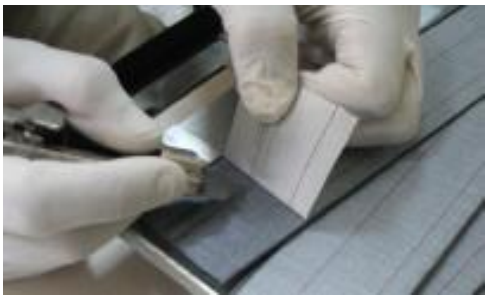

Figure 5: Peeling CFRP plate protective layer

2.5 Bonding Technique

Surface treatment is really important to produce good bonding because it will affect an adequate joint strength and produce adhesive failure. So, all the bond surfaces shall be properly treated prior to bonding. To produce a good bonding, the entire adherend bond surface shall be treated by following procedure:

i.) Solvent degreasing using a clean absorbent material which does not itself contaminates the surface.
ii.) Abraded using medium grit abrasive paper. Consideration at abrasive paper type must be taking into account before to be use with the suitable binder.
iii.) Degreasing shall be repeated.

During the surface roughening process, the pressure applied by the hand shall be adjusted to suitable condition as not to damage the outer adherend fibres. Commonly, it must be pretreated bonded together immediately after surface treatment to avoid contamination that can cause poor bonding, or if not possible the surface must be protected under suitable condition.

The bonding works start with the cleansing of concrete surface, as shown in Figure 6. The epoxy adhesive used is Sikadur-30 which is thixotropic adhesive mortar. The concrete prism was installed onto a specially made rig instrument for accurate bonding. A suitable amount of epoxy was applied onto the bonding surface and later the CFRP plate was pressed onto the epoxy as shown in Figure 7. Excessive epoxy was removed and the edges were chamfered. An imposed load was applied as shown in Figure 8 to ensure good bonding between the plates and concrete during hardening of the epoxy adhesive. The same procedures also applied to steel plate bonding process.

Figure 6: Surface cleansing to remove dust using compress air

Figure 7: Bonding CFRP Plate to concrete

Figure 8: Jig used for proper bonding

2.6 Instrumentation and Test Set-Up

Prior to the installation of strain gauges, the roughening process of CFRP and steel plates' surface using sand paper grade 400 was performed. In order to remove the dirt, Fast Dry Precision Cleaner Solvent was used on the CFRP plate and acetone on steel plates. The strain gauges were positioned at -50 mm, 15 mm, 35 mm, 65 mm, 105 mm and 155 mm apart as shown in Figure 9. After the installation process, the gauges were left for 24 hours for curing before testing. Later, an extension wires were joined to the gauge terminal by shouldering method. Figure 10 shows the test set-up for concrete prism, CFRP and steel plates. A direct tensile force was applied vertically and strain gauges were connected to data logger type TDS-302 where strain readings are recorded.

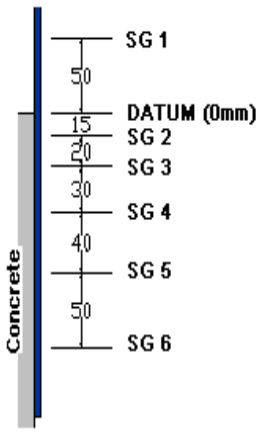

Figure 9: Strain gauges locations along bond length

Figure 10: Jig for Pull out Test for CFRP-concrete bonding

3.0 Results and Discussion

This section presents all the collected and tabulated data in table and graph forms. The rate of extension was set at 1.0 mm/min. Strain gauges readings were taken at an interval of every 5 kN. To simplify the analysis of test data, the bonding between CFRP plate and concrete prism was assumed to be perfect (i.e. no slip). Both adherents' materials were considered to be rigid creating a constant and uniform shear stress along the thickness of the epoxy adhesive. The adhesive was only be subjected to shear stress along the bond length and all materials involved were subjected to tensile loading up to failure.

3.1 CFRP Plate-Epoxy-Concrete Sample

Two samples had been tested for this particular group. Table 4 shows that the total applied failure loads for sample 1 and 2 namely CFRP/Con 1 and CFRP/Con 2 were 75.80 kN and 72.65 kN, respectively. The comparison between load versus extension and load versus time for both samples are shown in Figure 11 and Figure 12, respectively while the comparisons for the load strain at SG 1, SG 2, SG 4 and SG 6 in between both samples are shown in Figure 13.

Table 4: Relationship between time, extension and load of CFRP/Con 1 and CFRP/Con 2

Time	Extension (mm)		Load (kN)	
(s)	CFRP/Con 1	CFRP/Con 2	CFRP/Con 1	CFRP/Con 2
0	0	0	0	0
50	0.83	0.83	10.44	5.39
100	1.67	1.67	25.62	17.47
150	2.50	2.50	43.47	33.64
200	3.33	3.33	61.98	51.79
250	4.17	4.17	75.77	65.89
275	-	4.59	-	72.62
Max	4.17 (250.3 s)	4.60 (276.15 s)	75.80 (250.3 s)	72.65 (276.15 s)

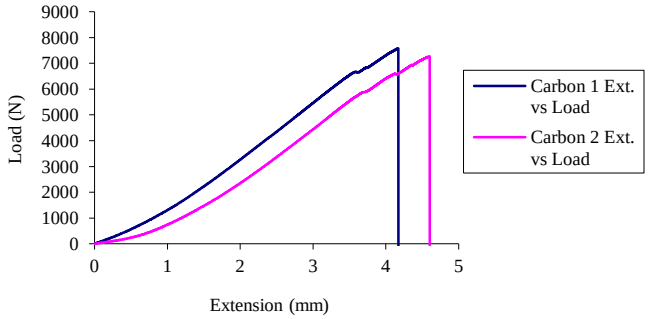

Figure 11: Load versus extension for CFRP/Con samples

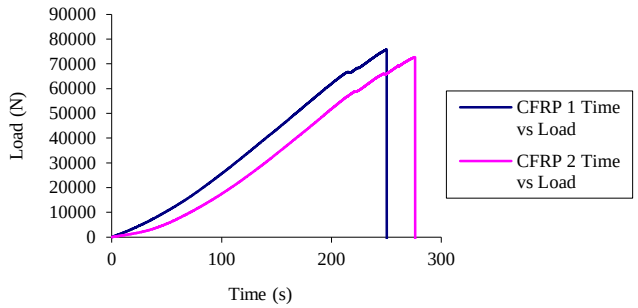

Figure 12: Load versus time for CFRP/Con samples

At the time interval of 225 seconds to 250 seconds and the extension of 3.5 mm to 4mm as shown in Figure 11 and Figure 12 respectively, it was clear that there were some disturbance with a minor drop of loadings at the end of the graphs. These signs implied that the concrete shearing started to occur before the samples were ruptured.

The comparisons for the load strain at SG 1, SG 2, SG 4 and SG 6 in between both samples were shown in Figure 13. The graph of total applied load versus local CFRP strain for CFRP/Con 1 was agreed to CFRP/Con 2. For both samples, it can be clearly seen that the strain distribution along the bond length was fairly linear, i.e. proportional to the applied load and uniform but with further increase of loads, the local strain became non-uniform and non-linear. The distance of the strain gauges along the bonding surface indicated bond stress distributions. SG 1, which was 50 mm on top of the datum, was linear throughout the test but the curve for SG 2 to SG 4 showed that stress distributions were quite critical along the first 65 mm of the bonding zone. SG 6 only sustains little stress.

Referring to Figure 13, it was found that the strain curves for both CFRP Plate-Epoxy-Concrete specimens work in the same manner even though both specimens failed at different sides. Differences were only detected once the tensile load reached around 55 kN.

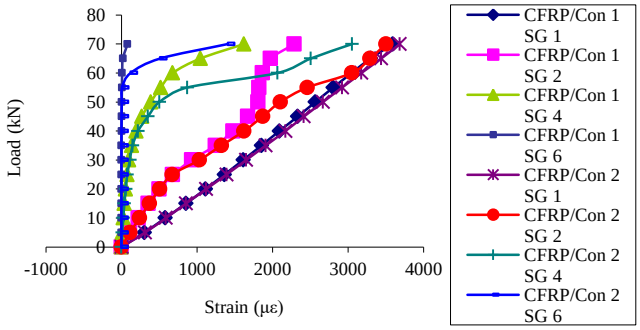

Figure 13: Load vs. strain comparison for CFRP Plate-Epoxy-Concrete Specimens

At the time of failure as shown in Figures 14 to 17, high strain energy was released and followed by a very loud sound generated. The failure started with the formation of cracking sound, indicating micro-debonding failure which probably occurred at the epoxy-concrete interface of the specimen. The full debonding started after the formation of macro-cracking at bond interface. The full bond failure had occurred in a very short period (i.e. less than one second) that indicated the sign of brittleness of the bond materials. It was also found that the debonding failure was dominated by concrete shearing failure which showed the weakness of concrete in shear or tensile properties compared to epoxy adhesive and CFRP plate composite.

By referring to the failure, it can be seen that a full concrete shearing failure had occurred on one side, while the occurrence of failure for the attached side was due to unbalance load imposed on the specimen just after total debonding. It was also noticed that no epoxy adhesive remained on the concrete surface, meaning to say that the epoxy adhesive was much stronger than concrete under shear deformation. It could be concluded that the full debonding of CFRP plate-epoxy from epoxy-concrete interfaces was due to an excessive interfacial shear stress that developed at epoxy-concrete interface.

Figure 14: Typical brittle bond failure for CFRP/Con 1

Figure 15: Concrete shearing for CFRP/Con 1

Figure 16: Typical brittle bond failure for CFRP/Con 2

Figure 17: Concrete shearing for CFRP/Con 2

3.2 Steel Plate-Epoxy-Concrete Sample

A sample with end tab applied on both sides of the sample for bonding of steel plates and concrete prism was tested until failure. Data collected and presented as in Table 5 showed that the total applied failure load for the sample namely Steel/Con 1 was 83.66 kN with maximum extension was 4.17 mm at 273.2 s of time.

Table 5: Relationship between time, extension and load of Steel/Con 1

Time (s)	Extension (mm)	Load (kN)
0	0	0
50	0.83	11.52
100	1.67	29.74
150	2.50	50.89
200	3.33	72.87
250	4.17	82.21
Max	4.17	83.66
	(273.2 s)	(273.2 s)

Generally, high stresses always occurred at the location of 0 to 60 mm of bond length. Sample Steel/Con 1 did not fail at bonding region but failed due to yielding of steel plates. The steel plates yielded at maximum load of 83.65 kN. Dividing the applied load by two, the estimated yielding load of the steel plate on average was 40.30 kN. The maximum extension for the specimen reached 4.17 mm at 273.2 s. It could be concluded that the steel plates started to yield at 83.60 kN and the welding of end plates only prevented the welded parts from yielding but the portions that were not welded continued to yield when pulled. The sample sustain a little bit more tensile load until the yielding of the steel plates was detected.

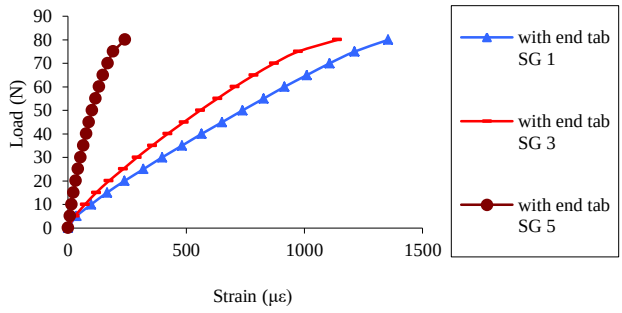

Figure 18: Load vs. strain comparison for Steel/Con 1

The strain distribution along the bond length was almost linear, i.e. proportional to the applied load and uniform. The comparisons at SG 1, SG 3, and SG 5 for both specimens were made as shown in Figure 18. It was found that the strain curves for both Steel Plate-Epoxy-Concrete specimens work in the same manner for SG 1 and SG 3. Differences were detected at SG 5 for the specimen most probably due to uneven and dissimilar concrete surface roughness that was formed during surface preparation. Adding extra end tabs only prevented the yielding at connection hole.

To justify the above mentioned statements, two steel plates were used for direct tensile test and it was found that both steel plates yield at approximately 41 kN or 82 kN at both directions. Therefore, it was concluded that the strength of steel plates used for this study was not sufficient in term of strength.

3.3 Bonding Behavior

The distance of the strain gauges along the bonding surface indicated the bond stress distributions. It was assumed that the bonding between the CFRP plate and concrete prism was perfect. The local stress and force transfer length at specific load level along the bond length was calculated and analysed from the local plate strains data.

From the plotted graph as shown in Figure 19, it was clear that CFRP plates performed better if compared to the steel plates. Stress concentration was quite close at SG 2 and SG 3. From SG 4 to SG 6, the stresses decreased gradually.

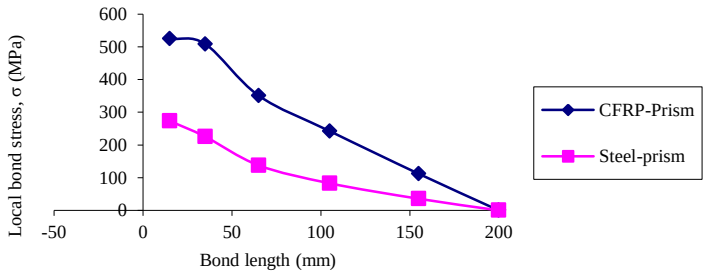

Figure 19: Local bond stress versus bond length comparison between CFRP/Con (average) and Steel/Con samples

The load versus strain relationships between CFRP-concrete and steel-concrete prisms were studied as shown in Figure 20. The strain distribution was more linear for steel-concrete prism specimen. Strain decreased gradually from SG 1 to SG 6. For CFRP-concrete prism specimen, the curves for SG1 and SG 2 were linear. From SG 4 to SG 6, it was found that the curves were non-linear form towards the ultimate load, indicating a

sudden load transfer from the front to the back of the plate due to debonding at the frontier region.

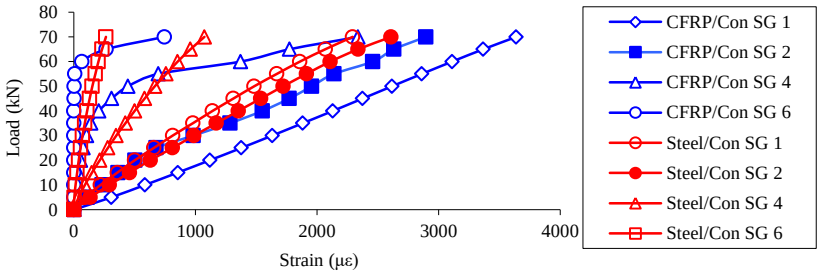

Figure 20: Load vs. strain comparison for between CFRP-Concrete and Steel-Concrete

4.0 Conclusions

From the results obtained, both materials bonded to concrete show different behavior in terms of bonding stress transfer.

For CFRP plates to concrete specimen, the bond force transfer at low load level was fairly linear and occurred at uniform rate but as the load level was near to failure, the bond force become non-linear with local debonding initiating at the specimen's highly loaded end. Bond failure for both specimens was dominant by the concrete shearing due to low shear properties of concrete compared to epoxy, CFRP and steel. All CFRP plates to concrete were term as perfect bonding where none of the specimen slipped between epoxy and concrete surface or epoxy and CFRP plates throughout the studies. The surface preparation was sufficient in providing good bonding between CFRP and concrete. The epoxy resin was indeed an ideal structural adhesive where bond failure was dominant by concrete shearing.

For steel plates to concrete sample, the bond force transfer from steel plate to concrete was linear and occurred at uniform rate. At higher load level, the steel plate started to yield at the connection holes where high stress concentration occurs before the debonding actually took place at the bonding surface. However, the existence of welded steel end tab at the connection region of the specimen sustain a little bit more tensile load until the yielding of the steel plates was detected The epoxy bonding was indeed stronger than the steel and the surface preparation was sufficient in providing good bonding between steel and concrete. Besides the tendency of surface slippages, the thickness of the steel plate was insufficient to carry the tensile load. A thicker and more durable steel plate need to be used with alternative surfacing techniques if available in future study.

The bonding strength was affected by the length of the bonding surface, modulus of elasticity of the materials and interfacial conditions. It is proven by the better performance from CFRP-prism samples with 283.2MPa local bond stress maximum differences if compared with the Steel-prism. Stress concentration was quite close at bond length of 15mm to 35mm. The stresses decreased gradually from bond length of 65mm to 155mm The longer or wider the bonding surface, the stronger the bonding strength would be but had to be limited to effective bond length of 60 mm to 120 mm.

5.0 Acknowledgements

The authors acknowledge Ministry of Higher Education Malaysia and Universiti Teknologi Malaysia for financial support through grant No. Q.J130000.2409.03G00, Development of Advanced Disaster Relief Utility Vehicle.

References

Abdel-Jaber, M. S., Walker, P. R., and Hutchinson, A. R. (2003). Shear Strengthening of Reinforced Concrete Beams Using Different Configurations of Externally Bonded Carbon Fibre Reinforced Plates. *Materials and Structures*, *36*(June), 291–301.

Abu Hassan, S., Gholami, M., Ismail, Y. S., and Mohd Sam, A. R. (2015). Characteristics of Concrete / CFRP Bonding System Under Natural Tropical Climate. *Construction and Building Materials*, *77*(July), 297–306.

Adhikary, B. B., and Mutsuyoshi, H. (2004). Behavior of Concrete Beams Strengthened in Shear with Carbon-Fiber Sheets. *Journal of Composites for Construction*, *8*(June), 258–264.

Al-Saawani, M. a., El-Sayed, a. K., and Al-Negheimish, a. I. (2015). Effect of Basic Design Parameters on IC Debonding of CFRP-Strengthened Shallow RC beams. *Journal of Reinforced Plastics and Composites*, *34*(18), 1526–1539.

Biscaia, H. C., Chastre, C., and Silva, M. a. G. (2015). Bond-Slip Model for FRP-to-Concrete Bonded Joints Under External Compression. *Composites Part B: Engineering*, *80*, 246–259.

British Standard Institution. (2009). BS EN 12390-3:2009. Testing Hardened Concrete. Compressive Strength of Test Specimens.

Burke, P. J., Bisby, L. a., and Green, M. F. (2013). Effects of Elevated Temperature on Near Surface Mounted and Externally Bonded FRP Strengthening Systems for Concrete. *Cement and Concrete Composites*, *35*(1), 190–199.

Christopher, K. Y. L. (2006). FRP Debonding from a Concrete Substrate: Some Recent Findings Against Conventional Belief. *Cement and Concrete Composites*, *28*, 742–748.

Daud, R. a., Cunningham, L. S., and Wang, Y. C. (2015). Static and Fatigue Behaviour of the Bond Interface between Concrete and Externally Bonded CFRP in Single Shear. *Engineering Structures*, *97*, 54–67.

De Domenico, D. (2015). RC Members Strengthened with Externally Bonded FRP Plates: A FE-Based Limit Analysis Approach. *Composites Part B: Engineering*, *71*, 159–174.

Deng, J., Lee, M. M. K., and Li, S. (2011). Flexural Strength of Steel–Concrete Composite Beams Reinforced with a Prestressed CFRP Plate. *Construction and Building Materials*, *25*(1), 379–384.

Deric J. Oehlers. (2001). Development of Design Rules for Retrofitting by Adhesive Bonding or Bolting Either FRP or Steel Plates to RC Beams or Slabs in Bridges and Buildings. *Composites, Part A*, *32*, 1345–1355.

Dong, J., Wang, Q., and Guan, Z. (2013). Structural behaviour of RC beams with external flexural and flexural–shear strengthening by FRP sheets. *Composites Part B: Engineering*, *44*(1), 604–612.

Firmo, J. P., Correia, J. R., Pitta, D., Tiago, C., and Arruda, M. R. T. (2015). Experimental Characterization of the Bond between Externally Bonded Reinforcement (EBR) CFRP Strips and Concrete at Elevated Temperatures. *Cement and Concrete Composites*, *60*, 44–54.

Fleming, C. J., and King, G. E. M. (1967). The Development of Structural Adhesives for Three Original Uses in South Africa. *Proc. RILEM Symp. Synthetic Resins in Building Construction, Paris, Sept. 1967*, 75–92.

Gao, B., Christopher, K. Y. L., and Kim, J.-K. (2007). Failure diagrams of FRP strengthened RC beams. *Composite Structures*, *77*, 493–508.

Gheorghiu, C., Labossiere, P., and Proulx, J. (2006). Fatigue and Monotonic Strength of RC Beams Strengthened with CFRPs. *Composites Part A: Applied Science and Manufacturing*, *37*, 1111–1118.

Gheorghiu, C., Labossiere, P., and Proulx, J. (2007). Response of CFRP-Strengthened Beams under Fatigue with Different Load Amplitudes. *Construction and Building Materials*, *21*, 756–763.

Grande, E., Imbimbo, M., and Sacco, E. (2011). Simple Model for Bond Behavior of Masonry Elements Strengthened with FRP. *Journal of Composites for Construction*, *15*(June), 354–363.

Hassan, S. A. (2007). *Mechanical Performance of Carbon Fibre Reinforced Vinyl Ester Composite Plate Bonded Concrete Exposed to Tropical Climate*. Universiti Teknologi Malaysia.

Juvandes, L. F. P., and Barbosa, R. M. T. (2012). Bond Analysis of Timber Structures Strengthened with FRP Systems. *Strain*, *48*(2), 124–135.

Kalfat, R., and Al-Mahaidi, R. (2015). Development of a Hybrid Anchor to Improve the Bond Performance of Multiple Plies of FRP Laminates Bonded to Concrete. *Construction and Building Materials*, *94*, 280–289.

Khalifa, A., Gold, W. J., Nanni, A., and Abdel Aziz, M. I. (1998). Contribution of Externally Bonded FRP to Shear Capacity of RC Flexural Members. *Journal of Composites for Construction*, *2*(4), 195–202.

Khelifa, M., Auchet, S., Méausoone, P.-J., and Celzard, A. (2015). Finite Element Analysis of Flexural Strengthening of Timber Beams with Carbon Fibre-Reinforced Polymers. *Engineering Structures*, *101*, 364–375.

Ko, H., Matthys, S., Palmieri, A., and Sato, Y. (2014). Development of a Simplified Bond Stress – Slip Model for Bonded FRP – Concrete Interfaces. *Construction and Building Materials*, *68*, 142–157.

Kotynia, R. (2012). Bond between FRP and Concrete in Reinforced Concrete Beams Strengthened with Near Surface Mounted and Externally Bonded Reinforcement. *Construction and Building Materials*, *32*, 41–54.

Mofidi, A., and Chaallal, O. (2011). Shear Strengthening of RC Beams with EB FRP: Influencing Factors and Conceptual Debonding Model. *Journal of Composites for Construction*, *15*(1), 62–74.

Seracino, R., Jones, N. M., Ali, M. S. M., Page, M. W., and Oehlers, D. J. (2007). Bond Strength of Near-Surface Mounted FRP Strip-to-Concrete Joints. *Journal of Composites for Construction*, *11*(August), 401–409.

Toutanji, H., and Ortiz, G. (2001). The Effect of Surface Preparation on the Bond Interface between FRP Sheets and Concrete Members. *Composite Structures*, *53*, 457–462.

Wang, F., Li, M., and Hu, S. (2014). Bond Behavior of Roughing FRP Sheet Bonded to Concrete Substrate. *Construction and Building Materials*, *73*, 145–152.

Wu, Z., Li, W., and Sakuma, N. (2006). Innovative Externally Bonded FRP/Concrete Hybrid Flexural Members. *Composite Structures*, *72*, 289–300.

Xu, T., He, Z. J., Tang, C. a., Zhu, W. C., and Ranjith, P. G. (2015). Finite Element Analysis of Width Effect in Interface Debonding of FRP Plate Bonded to Concrete. *Finite Elements in Analysis and Design*, *93*, 30–41.

Zheng, X. H., Huang, P. Y., Chen, G. M., and Tan, X. M. (2015). Fatigue Behavior of FRP–Concrete Bond Under Hygrothermal Environment. *Construction and Building Materials*, *95*, 898–909.